Eidgenössische Technische Hochschule Zürich

Ecole polytechnique fédérale de Zurich
Politecnico federale di Zurigo
Swiss Federal Institute of Technology Zurich

Sparse tensor finite elements for elliptic multiple scale problems*

H. Harbrecht† and Ch. Schwab

Research Report No. 2010-34
October 2010

Seminar für Angewandte Mathematik
Eidgenössische Technische Hochschule
CH-8092 Zürich
Switzerland

*Research of HH supported in part by DFG SimTech Cluster of Excellence; research of CS supported in part by ERC AdG Project 247277 STAHDPDE

†Institut für Angewandte Analysis und Numerische Simulation, Universität Stuttgart, Pfaffenwaldring 57, 70569 Stuttgart, Germany

Sparse tensor finite elements for elliptic multiple scale problems[☆]

Helmut Harbrecht[a,*], Christoph Schwab[b]

[a] *Institut für Angewandte Analysis und Numerische Simulation, Universität Stuttgart, Pfaffenwaldring 57, 70569 Stuttgart, Germany*
[b] *Seminar für Angewandte Mathematik, Eidgenössische Technische Hochschule Zürich, Rämistr. 101, 8092 Zürich, Switzerland*

Abstract

Locally periodic, elliptic multiscale problems in a bounded Lipschitz domain $D \subset \mathbb{R}^n$ with $K \geq 2$ separated scales are reduced to an elliptic system of K coupled, anisotropic elliptic one-scale problems in a cartesian product domain of total dimension Kn (e.g. (2; 3; 11; 26)). In (23; 31), it has been shown how these coupled elliptic problems could be solved by sparse tensor wavelet Finite Element methods in log-linear complexity with respect to the number N of degrees of freedom required by multilevel solvers for elliptic one-scale problems in D with the same convergence rate. In the present paper, the high dimensional one-scale limiting problems are discretized by a sparse tensor product finite element method (FEM) with standard, one-scale FE basis functions as used in engineering FE codes. Sparse tensorization and multilevel preconditioning is achieved by a BPX multilevel iteration.

We show that the resulting sparse tensor multilevel FEM resolves all physical length scales throughout the domain, with efficiency (i.e., accuracy versus work and memory) comparable to that of multigrid solvers for elliptic one-scale problems in the physical domain D. In particular, our sparse tensor FEM gives numerical approximations of the correct homogenized limit as well as compressed numerical representations of all first order correctors, throughout the physical domain with performance independent of the physical problem's scale parameters. Numerical examples with standard FE shape func-

[☆]Research of HH supported in part by DFG SimTech Cluster of Excellence; research of CS supported in part by ERC AdG Project 247277 STAHDPDE.

[*]Corresponding author

Email addresses: harbrecht@ians.uni-stuttgart.de (Helmut Harbrecht), schwab@sam.math.ethz.ch (Christoph Schwab)

tions and BPX multilevel preconditioners for elliptic problems with $K = 2$ separated, physical scales in spatial dimension $n = 2$ confirm the theoretical results. In particular, the present approach allows to avoid the construction of wavelet FE bases necessary in previous work (23; 31) while achieving resolution of all scales throughout the physical domain in log-linear complexity, with the logarithmic exponent behaving linearly in the number K of scales.

Keywords: Multiscale elliptic boundary value problem, reiterated homogenization, two-scale convergence, sparse tensor product FEM, BPX multilevel preconditioner, frames.

1. Introduction

Partial differential equations whose solutions exhibit multiple spatial and temporal length scales are ubiquitous models in engineering and in the sciences. Direct numerical resolution of all scales inherent in the solution is usually prohibitive, even on advanced computing hardware. There are two approaches to deal with multiple scales: the *modelling approach* and the *multiscale numerics approach*. The modelling approach replaces ("models") the mathematical governing equations with multiple scales by *approximate governing equations* which exhibit only a single scale. The multiscale numerics approach aims at *scale robustness*, i.e., at *resolving all scales at accuracy versus computational complexity independent of the problem's scale parameters*.

The modelling approach is used, for example, in closure models in kinetic theory and turbulence or in homogenization theory where so-called "effective" or "averaged" equations are analytically derived prior to numerical computation. Multiscale numerical schemes have emerged in the past decade as a powerful alternative to the modelling approach. We mention only "HMM"-type methods for elliptic homogenization problems (see, e.g. (1) and the references there) and generalized FEM which encode the fine scale of the solution into special, problem adapted basis functions. These methods are, as a rule, *scale robust*, but require in general more work to achieve a given accuracy than comparable methods for one-scale problems.

In the present paper, we develop a scale robust Finite Element Method (FEM) for scale separated elliptic multiscale problems in a bounded Lipschitz domain $D \subset \mathbb{R}^n$. Besides being scale robust, moreover, we prove that the complexity of the proposed FEM equals, up to logarithmic terms, that of a multilevel solver for an elliptic one-scale problem in D.

Our approach is based on the observation that solutions of elliptic multiscale problems can be completely described as solutions of elliptic one-scale problems on high dimensional domains. More recently, in (11–13) and the

references there, the "unfolding" formalism towards two-scale convergence and reiterated homogenization developed in (2; 3) based on the pioneering (26), has been developed. This development revealed in particular that the high dimensional, anisotropic elliptic one-scale problems arise *generically* (even in nonlinear problems when "homogenization formulas" and upscaling are not available) as characterizations of one-scale limits of elliptic multiscale problems: roughly speaking, *elliptic multiscale problems in n spatial dimensions with K separated scales result in "unfolded",* anisotropic and high-dimensional *elliptic one-scale problems in dimension nK*, i.e., *in computations, multiple spationtemporal scales can be traded for high dimension.*

As we observed in (23; 30) the natural idea of a Galerkin discretization of these high-dimensional, one-scale, "unfolded" elliptic limit problems on the tensor product of the physical domain D and $K-1$ unit-cells $Y \subset \mathbb{R}^n$ is hampered[1] by the fact that a straightforward discretization by tensor product finite elements with optimal, linear complexity solvers would yield scale robust solvers which require, however, $\mathcal{O}(h^{-Kn})$ degrees of freedom which is suboptimal for $K > 1$. Here, $\mathcal{O}(\cdot)$ is independent of ε and h denotes the mesh width of a shape regular, simplicial finite element mesh on $D \times Y \times \cdots \times Y$.

Hierarchical Finite Element bases, such as wavelet or multilevel bases, are used to build sparse tensor product FE spaces (see, e.g., (8; 18; 23; 31; 37)). On complicated domains of engineering interest the construction of Riesz bases of Finite Element type which respect essential boundary conditions is a nontrivial task. In the present work, we therefore show that multilevel frames based on standard, one scale finite elements admit spare tensor constructions. We propose a new, sparse tensor Finite Element algorithm and prove that it allows to approximate the homogenized solution and all interactions ("correctors") between the K length scales in the physical solution in essentially the complexity required to discretize an elliptic one-scale problem in $D \subset \mathbb{R}^n$, i.e., in work and memory $\mathcal{O}(h^{-n}|\log(h)|^{\alpha})$ with some $\alpha > 0$.

The basis of our frame construction are two[2] families of nested finite element spaces

$$U_0 \subset U_1 \subset U_2 \subset \cdots \subset H^1(D), \quad V_0 \subset V_1 \subset V_2 \subset \cdots \subset H^1_{\text{per}}(Y) \qquad (1)$$

as used in any multilevel scheme.

On a polyhedron $D \subset \mathbb{R}^n$ resp. on the unit cell $Y = [0,1]^n$, multilevel subspace sequences (1) are built by the standard procedure of uniformly

[1]For ease of exposition, we assume that all unit cells coincide with $Y = [0,1]^n$; analogous results are available for distinct unit cell geometries on each scale.

[2]Different unit cell geometries imply a separate multilevel hierarchy at each scale.

refining initial, regular simplicial triangulations of the domains D and Y. Unless stated explicitly otherwise, we assume that our Finite Elements are regular, affine families in the sense of Ciarlet (10). In case of curved domains we employ parametric finite elements to realize (1). The construction of parametric finite elements is based on a decomposition of the given domain into (curved) simplicial patches and suitable diffeomorphisms between the reference simplex and these patches. Uniform refinement of the reference simplex will lead then to a nested mesh of the domain. On each patch hierarchic families of simplicial finite elements are defined by transporting affine, simplicial families to the patch via parametrizations; parametrizations of adjacent patches are assumed to be C^0-compatible, so that subspaces and basis functions are assumed to match continuously across patch boundaries. The push-forward and pull-back operators, required in finite element based methods, can be derived from the underlying diffeomorphisms.

The outline of the paper is as follows. Section 2 introduces the homogenization problem under consideration and the related one-scale limiting problem. Section 3 is concerned with the full tensor product discretization by finite elements. The sparse tensor product discretization by multilevel frames is introduced and investigated in Section 4. Numerical results for elliptic two-scale problems are presented in Section 5. Finally, we state concluding remarks in Section 6.

Throughout the paper, in order to avoid the repeated use of generic but unspecified constants, by $C \lesssim D$ we mean that C can be bounded by a multiple of D, independently of parameters which C and D may depend on. Obviously, $C \gtrsim D$ is defined as $D \lesssim C$, and $C \sim D$ as $C \lesssim D$ and $C \gtrsim D$.

Acknowledgement. The paper was completed at the Institute for Mathematics and Its Applications, University of Minnesota, during the workshop *Computing with Uncertainty: Mathematical Modeling, Numerical Approximation and Large Scale Optimization of Complex Systems with Uncertainty* from October 18–22, 2010. The excellent working conditions at the IMA are gratefully acknowledged.

2. Elliptic K-scale problem

We formulate the elliptic homogenization problem with K scales and state the limiting problem as well as an error estimate between the solution of the limiting problem and the solution of the physical problem.

2.1. Problem formulation

In a bounded Lipschitz domain $D \subset \mathbb{R}^n$, and in $K-1$ unit cells $Y_1, \ldots, Y_{K-1}$ for the $K-1 \geq 1$ fast scales of the problem, we assume given an $(n \times n)$-

matrix function A depending on $K \geq 2$ variables in the following fashion:

$$A(\mathbf{x}, \mathbf{y}_1, \ldots, \mathbf{y}_{K-1}) \in L^\infty\big(D, C_{\text{per}}(Y_1 \times \cdots \times Y_{K-1})\big)^{n\times n}_{\text{sym}}$$

where, for all $K > k \geq 1$, we denote by $C_{\text{per}}(Y_1 \times \cdots \times Y_k)$ the space of continuous functions $\phi(\mathbf{y}_1, \ldots, \mathbf{y}_k)$, which admit continuous, Y_i-periodic extensions to all of $\mathbb{R}^n$ with respect to each coordinate $\mathbf{y}_i$ for $i = 1, \ldots, k$. The matrix function A is assumed periodic with respect to $\mathbf{y}_i$ with identical[3] periods $Y_i = [0, 1]^n$ for each $i = 1, \ldots, K-1$. We assume that A is bounded and uniformly positive definite, i.e., that there is a constant $\gamma > 0$ such that for all $\boldsymbol{\xi} \in \mathbb{R}^n$

$$\gamma|\boldsymbol{\xi}|^2 \leq \boldsymbol{\xi}^\top A(\mathbf{x}, \mathbf{y}_1, \ldots, \mathbf{y}_{K-1})\boldsymbol{\xi} \leq \gamma^{-1}|\boldsymbol{\xi}|^2, \tag{2}$$

for all $\mathbf{x} \in D$ and $\mathbf{y}_k \in Y$, $k = 1, \ldots, K-1$. For a scale parameter $\varepsilon > 0$ and a source term $f \in L^2(D)$, we consider the Dirichlet problem

$$-\operatorname{div} A^\varepsilon \nabla u^\varepsilon = f \text{ in } D, \quad u^\varepsilon = 0 \text{ on } \partial D. \tag{3}$$

The $(n \times n)$-matrix A^ε is assumed to depend on ε with multiple scales in the following sense: there exist $K-1$ positive *scale functions* $\varepsilon_1, \ldots, \varepsilon_{K-1}$ of ε that depend monotonically and continuously on ε and that converge to 0 when $\varepsilon \to 0$. The coefficient A^ε in (3) is assumed to be *scale separated* in the sense that

$$\lim_{\varepsilon\to 0} \varepsilon_{i+1}/\varepsilon_i = 0 \quad \text{for all } i = 1, \ldots, K-2 \tag{4}$$

and for all $\mathbf{x} \in D$ and all $0 < \varepsilon < 1$

$$A^\varepsilon(\mathbf{x}) = A\left(\mathbf{x}, \frac{\mathbf{x}}{\varepsilon_1}, \ldots, \frac{\mathbf{x}}{\varepsilon_{K-1}}\right).$$

Mathematical homogenization is the study of the limit of u^ε when ε tends to 0. Various approaches to this end have been developed. The oldest one is comprehensively exposed in Bensoussan, Lions and Papanicolaou (5). It consists in performing a formal multiscale asymptotic expansion and then in the justification of its convergence using the energy method due to Tartar (36). A significant result obtained with this approach was the existence of a ($L^2(D)$-) limit $u(\mathbf{x})$ of u^ε and, more importantly, the *identification of a limiting, "effective" or "homogenized" elliptic problem in D satisfied by u.*

[3]This assumption is adopted for ease of exposition only; all that follows has verbatim analogues in the case that at each scale i, there is a distinct periodicity pattern Y_i.

This approach has been widely used mainly for homogenization problems involving two separated scales. For nonlinear problems or problems with multiple scales it can only solve a restricted class of problems and becomes very complicated (see (3) for details). Homogenization formulas characterizing the one-scale limiting problem are generally not available. Performing the asymptotic expansion and using the energy method, have been combined to a single and method of two-scale convergence (for two-scale problems) originally by Nguetseng (26) and developed further by Allaire (2) and generalized to multiscale convergence by Allaire and Briane (3). This was extended recently into the "unfolding" formalism towards multiscale problems by (11). Rather than aiming at derivation of a single-scale, homogenized equation, a single-scale multidimensional limiting equation still containing all "fast variables" is derived in (3; 11). This limiting problem does not contain the scale parameters but still contains, to leading order, complete information on the physical solution's oscillations on all length scales. Bypassing the analytical derivation of "effective" equations implies, however, the numerical solution of a single-scale problem on a high dimensional domain. We review next some known results on this limiting equation for which we develop below an efficient sparse tensor FEM.

2.2. High-dimensional limit problem

A key ingredient of homogenization of elliptic problems with multiple scales is the notion of multiscale convergence. We present the definition here, based on Allaire and Briane (3).

Definition 2.1 ((3, Definition 2.3))**.** A sequence $\{u^\varepsilon\}_\varepsilon \subset L^2(D)$ K-scale converges to $u_0(\mathbf{x}, \mathbf{y}_1, \ldots, \mathbf{y}_{K-1}) \in L^2(D \times Y_1 \times \ldots Y_{K-1})$ if

$$\lim_{\varepsilon\to 0} \int_D u^\varepsilon \phi\left(\mathbf{x}, \frac{\mathbf{x}}{\varepsilon_1}, \ldots, \frac{\mathbf{x}}{\varepsilon_{K-1}}\right) d\mathbf{x} = \int_D \int_{Y_1} \ldots \int_{Y_{K-1}} u_0(\mathbf{x}, \mathbf{y}_1, \ldots, \mathbf{y}_{K-1}) \phi(\mathbf{x}, \mathbf{y}_1, \ldots, \mathbf{y}_{K-1}) d\mathbf{x} d\mathbf{y}_1 \ldots d\mathbf{y}_{K-1}$$

for any function $\phi \in L^2\big(D, C_{\text{per}}(Y_1 \times \ldots \times Y_{K-1})\big)$.

The application of K-scale convergence to problem (3) lies in the following compactness result:

Theorem 2.2 ((3, Theorem 2.5))**.** *Under the assumption (4) of scale separation, from each bounded sequence $\{u^\varepsilon\}_{\varepsilon>0} \subset L^2(D)$ we can extract a subsequence which K-scale converges, as $\varepsilon \to 0$, to a function $u_0 \in L^2(D \times Y_1 \times \ldots \times Y_{K-1})$.*

The variational formulation of the K-scale limit is based on the space

$$\begin{aligned}\mathbf{V} &= \big\{(\phi_0,\{\phi_k\}) : \phi_0 \in H^1_0(D),\\ &\qquad \phi_k \in L^2\big(D\times Y_1\times\cdots\times Y_{k-1}, H^1_{\mathrm{per}}(Y_k)\big),\ k=1,\dots,K-1\big\}\\ &= H^1_0(D)\times\prod_{k=1}^{K-1}\left[L^2(D)\otimes\left(\bigotimes_{i=1}^{k-1}L^2(Y_i)\right)\otimes H^1_{\mathrm{per}}(Y_k)\right] \qquad (5)\end{aligned}$$

endowed with the norm

$$\big\|(\phi_0,\{\phi_i\})\big\|_{\mathbf{V}} = \Big(\|\nabla\phi_0\|^2_{L^2(D)} + \sum_{k=1}^{K-1}\|\nabla_{\mathbf{y}_k}\phi_k\|^2_{L^2(D\times Y_1\times\cdots\times Y_k)}\Big)^{1/2} \qquad (6)$$

for $(\phi_0,\phi_1,\dots,\phi_{K-1})\in\mathbf{V}$ (in (5), tensor products over empty ranges of indices are skipped). The norm $\|\cdot\|_{\mathbf{V}}$ in (6) is anisotropic: it implies the control of first derivatives only in $\mathbf{y}_k$ of u_k, $k=1,2,\dots,K-1$. For the one-scale limit of problem (3) holds

Theorem 2.3. *As $\varepsilon\to 0$ in* (3)*, the solutions u^ε of* (3) *converge weakly in $H^1_0(D)$ to a function $u_0\in H^1_0(D)$ and the gradient ∇u^ε K-scale converges to the limit*

$$\nabla u_0(\mathbf{x}) + \sum_{k=1}^{K-1}\nabla_{\mathbf{y}_k}u_k(\mathbf{x},\mathbf{y}_1,\dots,\mathbf{y}_k).$$

Here, the function $u_0(\mathbf{x})$ is the homogenized solution. The vector function $(u_0,\{u_k\}) = (u_0,u_1,\dots,u_{K-1})$ of u_0 and of the scale interaction terms *$u_1,\dots,u_{K-1}$ is independent of ε. It can be obtained as the unique solution in the space $\mathbf{V}$ of the "unfolded", limiting variational problem: find $(u_0,\{u_k\})\in\mathbf{V}$ such that*

$$\begin{aligned}&b\big((u_0,\{u_i\}),(\phi_0,\{\phi_i\})\big)\\ &\quad= \int_D\int_{Y_1}\dots\int_{Y_{K-1}} A\Big(\nabla_{\mathbf{x}}u_0 + \sum_{i=1}^{K-1}\nabla_{\mathbf{y}_i}u_i\Big)\\ &\qquad\qquad\cdot\Big(\nabla_{\mathbf{x}}\phi + \sum_{j=1}^{K-1}\nabla_{\mathbf{y}_j}\phi_j\Big)d\mathbf{x}d\mathbf{y}_1\dots d\mathbf{y}_{K-1} = \int_D f\phi d\mathbf{x} \qquad (7)\end{aligned}$$

for all $(\phi_0,\{\phi_i\})\in\mathbf{V}$.

Under the ellipticity assumption (2)*, the bilinear form b is continuous and coercive in $\mathbf{V}$: there exist constants $c_1,c_2>0$ (depending only on D, K and on the coercivity constant $\gamma>0$ in* (2)*, but being independent of ε) such that*

$$b\big((u_0,\{u_i\}),(u_0,\{u_i\})\big) \ge c_1\big\|(u_0,\{u_i\})\big\|^2_{\mathbf{V}} \qquad (8)$$

for all $(u_0, \{u_i\}) \in \mathbf{V}$ *and*

$$b\big((u_0, \{u_i\}), (v_0, \{v_i\})\big) \leq c_2 \big\|(u_0, \{u_i\})\big\|_{\mathbf{V}} \big\|(v_0, \{v_i\})\big\|_{\mathbf{V}} \tag{9}$$

for all $(u_0, \{u_i\}), (v_0, \{v_i\}) \in \mathbf{V}$.

For a proof, we refer to (3, Theorem 2.11, Equation (2.9)).

Remark 2.4. The "unfolded" limit problem (7) is independent of the scale parameter ε, and is formulated in terms of the *a-priori known* coefficient A of the physical problem (3). Its (numerical) solution will yield the homogenized limiting solution u_0 without explicit knowledge of the coefficients of the homogenized equation; from the vector function $(u_0, u_1, \ldots, u_{K-1})$ the "effective" coefficient $A_0(\mathbf{x})$ of the homogenized limiting equation

$$-\operatorname{div}\big(A_0(\mathbf{x})\nabla u_0\big) = f \text{ in } D, \quad u_0 = 0 \text{ on } \partial D$$

satisfied by $u_0(\mathbf{x})$ can be obtained numerically if this is so desired.

Convergence of $u^\varepsilon \to u_0$ is strongly in $L^2(D)$, but only weak in $H^1(D)$, since information on the oscillations is lost in passing to the homogenized limit. This information is, to leading order, completely encoded in the scale interaction terms $u_1, \ldots, u_{K-1}$, as becomes clear from the following corrector result. It makes precise the way in which the scale interaction terms $(u_1, \ldots, u_{K-1})$ account for the oscillations of u^ε at small, positive values of ε.

Theorem 2.5 ((3, Theorem 2.14))**.** *Assume that the solution* $(u_0, u_1, \ldots, u_{K-1})$ *of problem (7) is sufficiently smooth, say* $u_0 \in C^1(\overline{D})$ *and* $u_k \in C^1\big(\overline{D}, C^1_{\mathrm{per}}(Y_1 \times \ldots \times Y_k)\big)$ *for all* $k = 1, \ldots, K-1$. *Then*

$$\left\| u^\varepsilon(\mathbf{x}) - \left[u(\mathbf{x}) + \sum_{k=1}^{K-1} \varepsilon_k u_k\left(\mathbf{x}, \frac{\mathbf{x}}{\varepsilon_1}, \ldots, \frac{\mathbf{x}}{\varepsilon_k}\right)\right]\right\|_{H^1(D)} \to 0 \quad \textit{as} \quad \varepsilon \to 0.$$

Remark 2.6. If the data A, D, f are smooth then the functions u, u_k are all smooth. We can also pass to the limit for certain classes of non-smooth matrices A. This leads to lower regularity of u_k but nevertheless a corrector can always be found using the *inverse unfolding operator* due to Cioranescu et al. (11). Details about which matrices A are "admissible" may be found in (3) and (11).

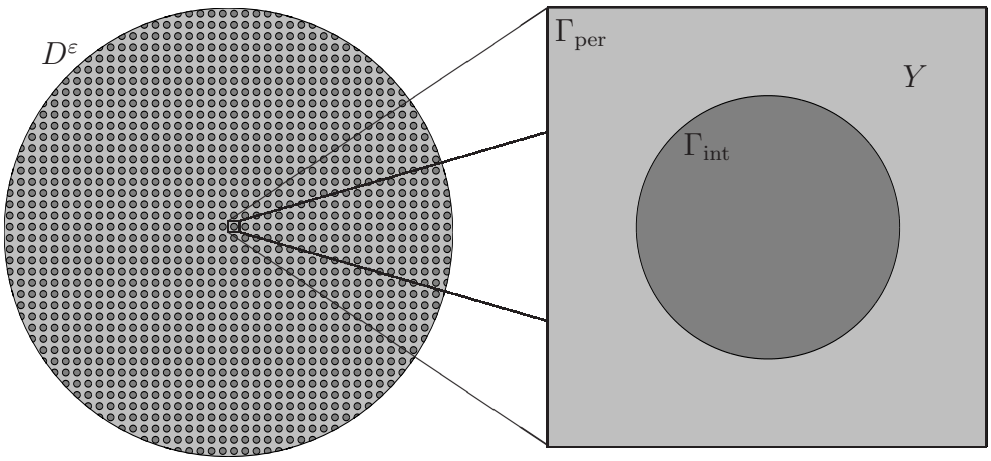

Figure 1: The domain D^ε with unit cell Y.

2.3. Two-scale problem

We develop the sparse tensor Finite Element discretization in the particular case of $K = 2$ scales and an isotropic coefficient, i.e., we consider the following elliptic homogenization problem in divergence form

$$-\operatorname{div}\left(A\Big(\mathbf{x},\frac{\mathbf{x}}{\varepsilon}\Big)\nabla u^\varepsilon(\mathbf{x})\right) = f(\mathbf{x}), \tag{10}$$

where the diffusion coefficient $A(\mathbf{x},\mathbf{y}) \in L^\infty(D\times Y)$ is assumed to be Y-periodic in the second variable $\mathbf{y}$ and uniformly positive

$$A(\mathbf{x},\mathbf{y}) \geq \gamma > 0 \quad \text{a.e. } (\mathbf{x},\mathbf{y}) \in D\times Y.$$

The unit cell $Y \subset [0,1]^n$ could be strictly included in $[0,1]^n$ in which case we assume the boundary

$$\partial Y = \Gamma_{\rm int} \cup \Gamma_{\rm per}, \quad \Gamma_{\rm per} := \partial Y \cap [0,1]^n, \quad \Gamma_{\rm int} := \partial Y \setminus \Gamma_{\rm per},$$

to be Lipschitz continuous. Notice that if $Y = [0,1]^n$ then $\Gamma_{\rm int} = \emptyset$. If $\Gamma_{\rm int} \neq \emptyset$ suitable boundary conditions have to be imposed at the boundary $\Gamma_{\rm int}$. We shall consider (10) in a bounded Lipschitz domain $D \subset \mathbb{R}^n$ covered by a pavement of cells of the form $\varepsilon(\mathbf{k}+Y)$ with $\mathbf{k} \in \mathbb{Z}^n$ and $\varepsilon/\operatorname{diam}(D) \ll 1$. We set

$$D^\varepsilon := D^\varepsilon_\infty \cap D, \text{ where } D^\varepsilon_\infty = \bigcup_{\mathbf{k}\in\mathbb{Z}^n} \varepsilon(\mathbf{k}+Y). \tag{11}$$

We indicate the various sets in the preceding definitions in Figure 1. We complete (10) in D^ε by homogeneous Dirichlet boundary conditions

$$u^\varepsilon = 0 \text{ on } \partial D. \tag{12}$$

2.4. Limit problem

Let $H^1_{\text{per}}(Y)$ denote the space of all $[0,1]^n$-periodic $H^1_{loc}(Y)$-functions. The space $\mathbf{V}$ in (5) for the variational formulation of the limiting problem reads

$$\begin{aligned}\mathbf{V} &:= \big\{(w_0, w_1) : w_0 \in H^1_0(D),\ w_1 \in L^2\big(D; H^1_{\text{per}}(Y)/\mathbb{R}\big)\big\} \\ &\simeq H^1_0(D) \times L^2\big(D; H^1_{\text{per}}(Y)/\mathbb{R}\big).\end{aligned}$$

We note that by Fubini's Theorem, the Bochner-type function space for the scale interaction term u_1 is isomorphic to a tensor product space, i.e.

$$L^2\big(D; H^1_{\text{per}}(Y)/\mathbb{R}\big)\big) \simeq L^2(D) \otimes \big(H^1_{\text{per}}(Y)/\mathbb{R}\big) \tag{13}$$

where $\otimes$ denotes the tensor product of separable Hilbert spaces. Accordingly, the expression

$$\|(u_0, u_1)\|_{\mathbf{V}} = \Big(\|\nabla_{\mathbf{x}} u_0\|^2_{L^2(D)} + \|\nabla_{\mathbf{y}} u_1\|^2_{L^2(D\times Y)}\Big)^{1/2}$$

is a norm on $\mathbf{V}$. On $\mathbf{V}$, the bilinear form $B(\cdot,\cdot)$ in the variational formulation of the limiting problem (7) takes the form

$$\begin{aligned}b\big((u_0, u_1), (v_0, v_1)\big) := \int_D \int_Y A(\mathbf{x}, \mathbf{y})\big(\nabla_{\mathbf{x}} u_0(\mathbf{x}) + \nabla_{\mathbf{y}} u_1(\mathbf{x}, \mathbf{y})\big) \\ \cdot \big(\nabla_{\mathbf{x}} v_0(\mathbf{x}) + \nabla_{\mathbf{y}} v_1(\mathbf{x}, \mathbf{y})\big) d\mathbf{y} d\mathbf{x}.\end{aligned} \tag{14}$$

By (8) and (9), for any given linear form

$$\ell : \mathbf{V} \to \mathbb{R}, \quad \ell(v_0, v_1) := \int_D f(\mathbf{x}) v_0(\mathbf{x}) d\mathbf{x},$$

the variational problem

$$\begin{aligned}&\text{find } (u_0, u_1) \in \mathbf{V} \text{ such that} \\ &\quad b\big((u_0, u_1), (v_0, v_1)\big) = \ell(v_0, v_1) \text{ for all } (v_0, v_1) \in \mathbf{V}\end{aligned} \tag{15}$$

admits a unique solution $(u_0, u_1) \in \mathbf{V}$. For the case of $K = 2$ scales which is under consideration here, the convergence result Theorem 2.5 of $u^\varepsilon \in H^1_0(D^\varepsilon)$ to the "folded" two-scale solution $(u_0, u_1) \in \mathbf{V}$ can be quantified in in the following sense: according to (5; 24) and (23, Theorem 4.1) holds the asymptotic error bound

$$\Big\| u_0 + \varepsilon u_1\Big(\cdot, \frac{\cdot}{\varepsilon}\Big) - u^\varepsilon \Big\|_{H^1(D^\varepsilon)} = \mathcal{O}(\sqrt{\varepsilon}), \tag{16}$$

provided that $A \in W^{1,\infty}(D; C^\infty_{\text{per}}(Y))$ and that $u_0 \in H^2(D)$.

3. Finite element discretization

3.1. Multiresolution analyses

Let $D \subset \mathbb{R}^n$ be a polygonal and bounded domain with coarse grid triangulation $\mathcal{T}_0 = \{\tau_{0,k}\}$. By uniform subdivision of each simplex on level $j-1$ into 2^n simplices on level j, we obtain recursively a nested family of simplicial triangulations $\mathcal{T}_j = \{\tau_{j,k}\}$ for all $j > 0$. On the triangulation $\mathcal{T}_j$ we define standard Lagrangian piecewise polynomial continuous finite elements $\Phi_j = \{\varphi_{j,k} : k \in \Delta_j\}$ (Δ_j denotes an appropriate index set) and obtain a nested sequence of finite dimensional trial spaces

$$V_0 \subset V_1 \subset \cdots \subset V_j \subset \cdots \subset H^1(D), \tag{17}$$

where

$$V_j = \operatorname{span}\{\varphi_{j,k} : k \in \Delta_j\} = \{u \in C(D) : u|_\tau \in \Pi_d \text{ for all } \tau \in \mathcal{T}_j\}$$

where $\dim V_j \sim 2^{jn}$. For our approach it is convenient to normalize the Lagrangian finite elements with respect to the energy space $H^1(D)$, i.e.,

$$\|\varphi_{j,k}\|_{H^1(D)} \sim 1. \tag{18}$$

The spaces V_j satisfy the following Jackson and Bernstein type estimates for all $s \le t < 3/2$, $t \le q \le d+1$

$$\inf_{v_j \in V_j} \|u - v_j\|_{H^t(D)} \lesssim h_j^{q-t} \|u\|_{H^q(D)}, \quad u \in H^q(D), \tag{19}$$

and

$$\|v_j\|_{H^t(D)} \lesssim h_j^{s-t} \|v_j\|_{H^s(D)}, \quad v_j \in V_j, \tag{20}$$

uniformly in j, where we set $h_j := 2^{-j}$. Here $h_j \sim \max_k\{\operatorname{diam} \tau_{j,k}\}$ denotes the mesh width of the subspace V_j on D.

3.2. Curved domains and parametric finite elements

In case of non-polygonal domains with piecewise smooth boundaries we can use parametric finite elements to realize the multiresolution analysis (17). We assume that the domain D is given as a collection of simplicial smooth patches. More precisely, let $\triangle$ denote the reference simplex in $\mathbb{R}^n$. We assume that the domain D is partitioned into M patches

$$\overline{D} = \bigcup_{k=1}^{M} \tau_{0,k}, \quad \tau_{0,k} = \boldsymbol{\kappa}_k(\triangle), \quad k = 1, 2, \ldots, M, \tag{21}$$

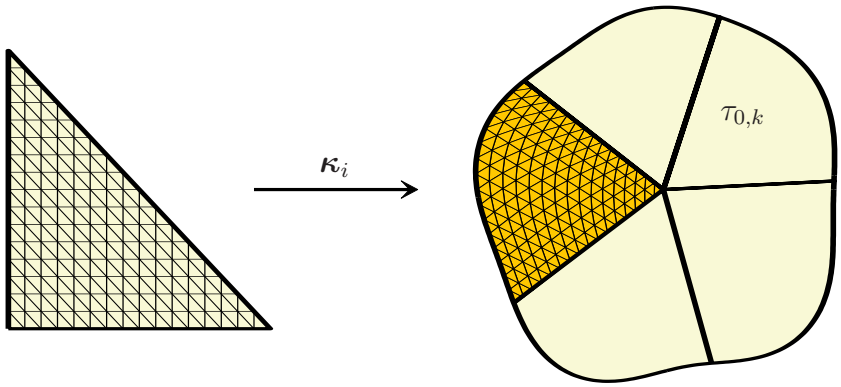

Figure 2: Construction of parametric finite elements

where each $\boldsymbol{\kappa}_k : \triangle \to \tau_{0,k}$ defines a diffeomorphism of $\triangle$ onto $\tau_{0,k}$. The intersection $\tau_{0,k} \cap \tau_{0,k'}$, $k \neq k'$, any two patches $\tau_{0,k}$ and $\tau_{0,k'}$ is supposed to be either $\emptyset$, or a lower dimensional face.

A mesh of level j on D is induced by regular subdivisions of depth j of the reference simplex into 2^{jn} sub-simplices. This generates the $2^{jn}M$ elements $\{\tau_{j,k}\}$. In order to ensure that the collection $\{\tau_{j,k}\}$ of elements on the level j forms a regular mesh on D, the parametrizations $\{\boldsymbol{\kappa}_k\}$ are assumed to be C^0 compatible in the following sense: a bijective, affine mapping $\boldsymbol{\Xi} : \triangle \to \triangle$ exists such that for all $\mathbf{x} = \boldsymbol{\kappa}_i(\mathbf{s})$ on a common interfaces of $\tau_{0,i}$ and $\tau_{0,i'}$ it holds that $\boldsymbol{\kappa}_i(\mathbf{s}) = (\boldsymbol{\kappa}_{i'} \circ \boldsymbol{\Xi})(\mathbf{s})$. In other words, the diffeomorphisms $\boldsymbol{\kappa}_i$ and $\boldsymbol{\kappa}_{i'}$ coincide at the common interface except for orientation. An illustration of such a triangulation is found in Fig. 2.

Finally, we define the Finite Element ansatz functions via the parametrizations $\{\boldsymbol{\kappa}_i\}$ in the usual fashion, i.e., by lifting Lagrangian finite elements from $\triangle$ to the domain D by using the mappings $\boldsymbol{\kappa}_i$. Continuous basis functions whose support overlaps with several patches are obtained by gluing across patch boundaries, using the C^0 interpatch compatibility. This yields a sequence of nested finite element spaces (17) that satisfy the same Jackson and Bernstein type estimates (19) and (20) as the standard finite element spaces from the previous subsection.

3.3. FEM discretization

Since we have to discretize two domains we need two dense families of nested Finite Element spaces

$$U_0 \subset U_1 \subset \cdots \subset U_j \subset \cdots \subset H^1(D), \quad U_j = \operatorname{span}\{\varphi_{j,k} : k \in \triangle_j^{\overline{D}}\},$$
$$V_0 \subset V_1 \subset \cdots \subset V_j \subset \cdots \subset H^1_{\mathrm{per}}(Y), \quad V_j = \operatorname{span}\{\psi_{j,k} : k \in \triangle_j^{Y}\}.$$

In order for the family $\{U_j\}_{j=0}^{\infty}$ to be conforming to $H^1_{\mathrm{per}}(Y)$, we assume that the corresponding sequence $\{\triangle_j\}_{j=0}^{\infty}$ is Y-periodic, i.e., the Y-periodic extension of $\triangle_j$ beyond the unit cell Y is a regular mesh in $\mathbb{R}^n$; this assumption forces compatibility of boundary nodes on ∂Y. We also assume that both types of ansatz spaces have the same approximation order d (see Remark 3.3 below). Moreover, to discretize functions in $H^1_0(D)$ we will remove the degrees of freedom associated with the boundary nodes which yields the multiscale hierarchy

$$U_0^\circ \subset U_1^\circ \subset \cdots \subset U_j^\circ \subset \cdots \subset H^1_0(D), \quad U_j^\circ = \operatorname{span}\{\varphi_{j,k} : k \in \triangle_j^D\}.$$

For sake of simplicity we shall assume that the diffusion coefficient is separable, i.e., that

$$A(\mathbf{x},\mathbf{y}) = \alpha(\mathbf{x})\beta(\mathbf{y}). \tag{22}$$

In the (practically more frequent) case of non-separable coefficients, we approximate $A(\mathbf{x},\mathbf{y})$ by a separable expansion

$$A(\mathbf{x},\mathbf{y}) = \sum_{i=1}^{M} \alpha_i(\mathbf{x})\beta_i(\mathbf{y}), \tag{23}$$

for example in terms of a truncated singular value decomposition.

If $A \in C^\infty\big(\overline{D}, C^\infty_{\mathrm{per}}(Y)\big)$, the error bound (16) holds, and for every M, a separated expansion (23) can be computed in essentially linear complexity by using the techniques from (34). For coefficient expansions (23) the following developments will be applied term-by-term. Setting

$$\begin{aligned}
b_1(u_0,v_0) &:= \int_D \int_Y \alpha(\mathbf{x})\beta(\mathbf{y})\nabla_{\mathbf{x}} u_0(\mathbf{x})\nabla_{\mathbf{x}} v_0(\mathbf{x}) d\mathbf{y} d\mathbf{x},\\
b_2(u_0,v_1) &:= \int_D \int_Y \alpha(\mathbf{x})\beta(\mathbf{y})\nabla_{\mathbf{x}} u_0(\mathbf{x})\nabla_{\mathbf{y}} v_1(\mathbf{x},\mathbf{y}) d\mathbf{y} d\mathbf{x},\\
b_3(u_1,v_1) &:= \int_D \int_Y \alpha(\mathbf{x})\beta(\mathbf{y})\nabla_{\mathbf{y}} u_1(\mathbf{x},\mathbf{y})\nabla_{\mathbf{y}} v_1(\mathbf{x},\mathbf{y}) d\mathbf{y} d\mathbf{x},
\end{aligned} \tag{24}$$

we arrive at (cf. (14))

$$b\big((u_0,u_1),(v_0,v_1)\big) = b_1(u_0,v_0) + b_2(u_0,v_1) + b_2(v_0,u_1) + b_3(u_1,v_1). \tag{25}$$

Next, we will introduce the system matrices for ansatz and test functions on arbitrary levels. Of course, in standard finite element methods supports of tensor-product shape functions are isotropic and, hence, the levels of ansatz and test functions are always the same. But later on, in the context of the sparse discretization scheme, this general situation will appear.

We will discretize $u_0 \in H_0^1(D)$ in the finite element space U_j° and $u_1 \in L^2(D) \otimes H^1(Y)$ in the tensor product space $W_j := U_j \otimes V_j$. To do so, in view of (22), we define the constant $\mathbf{c} := (\beta, 1)_{L^2(Y)}$, the matrices associated with the domain D

$$\begin{aligned}
\mathbf{G}_{j,j'} &:= \Big[(\alpha\varphi_{j',k'}, \varphi_{j,k})_{L^2(D)}\Big]_{k\in\triangle_j^{\overline{D}}, k'\in\triangle_{j'}^{\overline{D}}} \in \mathbb{R}^{|\triangle_j^{\overline{D}}|\times|\triangle_{j'}^{\overline{D}}|},\\
\mathbf{B}_{j,j'} &:= \Big[(\alpha\nabla\varphi_{j',k'}, \nabla\varphi_{j,k})_{L^2(D)}\Big]_{k\in\triangle_j^{D}, k'\in\triangle_{j'}^{D}} \in \mathbb{R}^{|\triangle_j^{D}|\times|\triangle_{j'}^{D}|},\\
\mathbf{F}_{j,j'}^i &:= \Big[(\alpha\varphi_{j',k'}, \partial_{x_i}\varphi_{j,k})_{L^2(D)}\Big]_{k\in\triangle_j^{D}, k'\in\triangle_{j'}^{\overline{D}}} \in \mathbb{R}^{|\triangle_j^{D}|\times|\triangle_{j'}^{\overline{D}}|}, \quad i = 1, 2, \ldots, n,
\end{aligned} \tag{26}$$

the matrices associated with the domain Y

$$\begin{aligned}
\mathbf{C}_{j,j'} &:= \Big[(\beta\nabla\psi_{j',k'}, \nabla\psi_{j,k})_{L^2(Y)}\Big]_{k\in\triangle_j^{Y}, k'\in\triangle_{j'}^{Y}} \in \mathbb{R}^{|\triangle_j^{Y}|\times|\triangle_{j'}^{Y}|},\\
\mathbf{b}_j^i &:= \Big[(\partial_{y_i}\psi_{j,k}, \beta)_{L^2(Y)}\Big]_{k\in\triangle_j^{Y}} \in \mathbb{R}^{1\times|\triangle_j^{Y}|}, \quad i = 1, 2, \ldots, n,
\end{aligned} \tag{27}$$

and the data vector

$$\mathbf{f}_j := \Big[(f, \varphi_{j,k})_{L^2(D)}\Big]_{k\in\triangle_j^{D}} \in \mathbb{R}^{|\triangle_j^{D}|\times 1}.$$

Then, by (24) and (25), the ansatz

$$\begin{aligned}
u_{0,j} &= \textstyle\sum_{k\in\triangle_j^{D}} [\mathbf{u}_{0,j}]_k \varphi_{j,k} \in U_j^\circ,\\
u_{1,j} &= \textstyle\sum_{k\in\triangle_j^{\overline{D}}} \sum_{k'\in\triangle_j^{Y}} [\mathbf{u}_{1,j}]_{k,k'} (\varphi_{j,k} \otimes \psi_{j,k'}) \in W_j,
\end{aligned} \tag{28}$$

leads to the following symmetric and positive definite linear system of equations

$$\begin{bmatrix} \mathbf{c}\mathbf{B}_{j,j} & \sum_{i=1}^n \mathbf{b}_j^i \otimes \mathbf{F}_{j,j}^i \\ \big(\sum_{i=1}^n \mathbf{b}_j^i \otimes \mathbf{F}_{j,j}^i\big)^\top & \mathbf{C}_{j,j} \otimes \mathbf{G}_{j,j} \end{bmatrix} \begin{bmatrix} \mathbf{u}_{0,j} \\ \mathbf{u}_{1,j} \end{bmatrix} = \begin{bmatrix} \mathbf{f}_j \\ \mathbf{0} \end{bmatrix}. \tag{29}$$

Remark 3.1. The constraint

$$\int_D \int_Y u_1(\mathbf{x}, \mathbf{y}) w(\mathbf{x}) d\mathbf{y} d\mathbf{x} = 0 \quad \text{for all} \quad w \in L^2(D)$$

is not discretized explicitly. The Galerkin solution $(u_{0,j}, u_{1,j})$ of (29) will satisfy the constraint since the right hand side lies in $\mathbf{V}$ and Krylov subspace solvers iterate orthogonal to the kernel (25), see also Subsection 4.3 for more details.

Céa's lemma together with the approximation property (19) gives rise to the following standard error estimate.

Proposition 3.2. *Assume $u_0 \in H_0^{1+s}(D)$ and $u_1 = H^{1+s}(D) \otimes H^{1+s}_{\mathrm{per}}(Y)/\mathbb{R}$ for some $0 \le s \le d$. Then, the sparse tensor FE approximation $(u_{0,j}, u_{1,j})$ given by (28), (29) satisfies the error estimate*

$$\begin{aligned}\|(u_0,u_1)-(u_{0,j},u_{0,j})\|_{\mathbf{V}} &\lesssim \inf_{(v_{0,j},v_{1,j})\in U_j\times W_j} \|(u_0,u_1)-(v_{0,j},v_{1,j})\|_{\mathbf{V}}\\ &\lesssim h_j^s\big\{\|u_0\|_{H^{1+s}(D)}+\|u_1\|_{H^s(D)\otimes H^{1+s}_{\mathrm{per}}(Y)}\big\}.\end{aligned}$$

Remark 3.3. It can be figured from this error estimate that it would be sufficient to employ finite elements of order $d-1$ to approximate in $L^2(D)$ with optimal rate, i.e., in the first coordinate of u_1. Nevertheless, we employ the same finite elements as in $H^1(D)$ in order to keep the notation simple.

4. Sparse tensor two-scale FEM

4.1. Sparse tensor product spaces

The finite element discretization of u_1 in the tensor product space $W_j := U_j \otimes V_j$ results in $\dim(U_j)\cdot\dim(V_j) \sim 2^{2jn}$ degrees of freedom which is prohibitively large. We approximate the "scale interaction function" u_1 in the *sparse tensor product space*

$$\widehat{W}_j := \widehat{U_j \otimes V_j} = \sum_{\ell+\ell'\le j} U_\ell \otimes V_{\ell'}.$$

It owns much less degrees of freedom than the full tensor product space W_j. Namely, there holds $\dim(\widehat{W}_j) \sim 2^{jn} j$, cf. (8). Consequently, the discretization of u_1 will have essentially the same number of unknowns as the discretization of u_0.

The following lemma from (23) (see also (28; 33)), implies that the approximation power in the sparse tensor product spaces is nearly as good as in the full tensor product spaces, provided that the given function has some extra regularity in terms of bounded mixed derivatives.

Lemma 4.1. *For $w \in H^t(D)\otimes H^{t+1}_{\mathrm{per}}(Y)$ for some $0 \le t \le d$ holds the error estimate*

$$\inf_{\widehat{w}_j\in\widehat{W}_J} \|w-\widehat{w}_j\|_{L^2(D)\otimes H^1_{\mathrm{per}}(Y)} \lesssim \begin{cases} 2^{jt}\sqrt{j}\|w\|_{H^t(D)\otimes H^{t+1}_{\mathrm{per}}(Y)}, & \text{if } t=d,\\ 2^{jt}\|w\|_{H^t(D)\otimes H^{t+1}_{\mathrm{per}}(Y)}, & \text{otherwise.}\end{cases}$$

4.2. Galerkin discretization

To approximate functions in $\widehat{W}_J$ one traditionally uses hierarchical bases like wavelet or multilevel bases, see for example (8; 17; 37). Here we will use multilevel frames as proposed in (22), i.e., we will represent functions by the redundant collection

$$\widehat{\Upsilon}_j := \big\{\varphi_{\ell,k} \otimes \psi_{\ell',k'} : k \in \Delta_\ell^{\overline{D}},\ k' \in \Delta_{\ell'}^{Y},\ \ell + \ell' \le j\big\}.$$

As one readily verifies it holds $\operatorname{span}\{\widehat{\Upsilon}_j\} = \widehat{W}_j$ and $\operatorname{card}(\widehat{\Upsilon}_j) \sim 2^{jn} j \sim \dim(\widehat{W}_j)$, i.e., this set has still optimal cardinality. We mention that the frame $\widehat{\Upsilon}_j$ is the restriction to $\widehat{W}_j$ of the tensor product of the frames which underly the BPX-preconditioners on D and Y (see (7; 15; 27)). For details concerning the frame theory we refer the reader to e.g. (9; 16; 35).

The frame $\widehat{\Upsilon}_j$ is stable in $H^s(D) \otimes H^t(Y)$ for all $0 < s, t < 3/2$ if the ansatz functions are properly scaled (22) (see also (20)). Since we need here the limit case $s = 0$ the stability constant grows logarithmically in the level index j, i.e., uniformly in j we have (cf. (22))

$$\begin{aligned} &\|f\|^2_{L^2(D)\otimes H^{-1}_{\mathrm{per}}(Y)} \\ &\qquad \lesssim \sum_{\ell+\ell' \le J} \sum_{k \in \Delta_\ell^{\overline{D}}} \sum_{k' \in \Delta_{\ell'}^{Y}} 2^{-\ell} (f, \varphi_{\ell,k} \otimes \psi_{\ell',k'})_{L^2(D\times Y)} \\ &\qquad\qquad \lesssim j \|f\|^2_{L^2(D)\otimes H^{-1}_{\mathrm{per}}(Y)} \end{aligned} \tag{30}$$

for all $f \in L^2(D) \otimes H^{-1}_{\mathrm{per}}(Y)$.

Then, similarly to (29), the ansatz

$$\begin{aligned} u_{0,j} &= \sum_{k \in \Delta_j^D} [\mathbf{u}_{0,j}]_k \varphi_{j,k} \in U_j^\circ, \\ \widehat{u}_{1,j} &= \sum_{\ell+\ell' \le j} \sum_{k \in \Delta_\ell^{\overline{D}}} \sum_{k' \in \Delta_{\ell'}^{Y}} [\widehat{\mathbf{u}}_{1,j}]_{(k,\ell),(k',\ell')} (\varphi_{\ell,k} \otimes \psi_{\ell',k'}) \in \widehat{W}_j \end{aligned}$$

yields the following linear system of equations

$$\begin{bmatrix} c\mathbf{B}_{j,j} & \sum_{i=1}^n \mathbf{b}_j^i \widehat{\otimes} \mathbf{F}^i_{j,j} \\ \big(\sum_{i=1}^n \mathbf{b}_j^i \widehat{\otimes} \mathbf{F}^i_{j,j}\big)^\top & \mathbf{C}_{j,j} \otimes \mathbf{G}_{j,j} \end{bmatrix} \begin{bmatrix} \mathbf{u}_{0,j} \\ \widehat{\mathbf{u}}_{1,j} \end{bmatrix} = \begin{bmatrix} \mathbf{f}_j \\ \mathbf{0} \end{bmatrix}. \tag{31}$$

Herein, the notion "$\widehat{\cdot}$" indicates the application of the frame which implies

$$\begin{aligned} \widehat{\mathbf{b}_j^i \otimes \mathbf{F}^i_{j,j}} &= \big[\mathbf{b}_{\ell_1} \otimes \mathbf{F}^i_{j,\ell_2}\big]_{\ell_1+\ell_2 \le j}, \\ \widehat{\mathbf{C}_{j,j} \otimes \mathbf{G}_{j,j}} &= \big[\mathbf{C}_{\ell_1,\ell_1'} \otimes \mathbf{G}_{\ell_2,\ell_2'}\big]_{\ell_1+\ell_2,\ell_1'+\ell_2' \le j}. \end{aligned} \tag{32}$$

Proposition 4.2. *The approximate solution* $(u_{0,j}, \widehat{u}_{1,j}) \in U_j \times \widehat{W}_j$ *from* (31) *satisfies the error estimate*

$$\begin{aligned}\|(u_0, u_1) - (u_{0,j}, \widehat{u}_{1,j})\|_{\mathbf{V}} &\lesssim \inf_{(v_{0,j}, \widehat{v}_{1,j}) \in U_j \times \widehat{W}_j} \|(u_0, u_1) - (v_{0,j}, \widehat{v}_{1,j})\|_{\mathbf{V}} \\ &\lesssim j h_j^{d-1} \big\{ \|u_0\|_{H^d(D)} + \|u_1\|_{H^{d-1}(D) \otimes H^d_{\mathrm{per}}(Y)} \big\}\end{aligned}$$

provided that the given data are sufficiently smooth.

Remark 4.3. By using wavelets, for example Haar wavelets, instead of the multilevel frame to discretize functions in $L^2(D)$, also the upper constant of (30) is independent of the level j. Consequently, the (generalized) condition number of the associated linear system of equations (31) would be independent of the level j. However, we avoided wavelets to keep the algorithms as simple as possible. Particularly our numerical results in Section 5 show that the logarithm in (30) behaves quite harmless.

4.3. Iterative solution of the linear systems of equations

Due to the non-uniqueness of the representation of functions in frame coordinates, the system matrix in (31) has a large kernel. However, the associated right hand side lies in the image of the system matrix. Thus, Krylov subspace methods converge without further modifications (see, e.g., (14; 17; 18; 25) for details). This is due to the Krylov subspace, and thus the residuum, staying orthogonal to the kernel. Here, the system (31) is symmetric. Hence, we can apply the conjugate gradient method. Applying the BPX-preconditioner (7) for the finite element part associated with u_0 and a diagonal scaling (by using the diagonals of the $\mathbf{C}_{\ell,\ell}$ and $\mathbf{G}_{\ell,\ell}$ which are easily accessible) for the unknowns of the sparse tensor product space, associated with u_1, the ratio of the nonzero eigenvalues of the system matrix will be essentially bounded independently of the mesh width. Therefore, the conjugate gradient method will converge with a rate that is essentially independent of the discretization level j at each physical length scale.

4.4. Prolongations and restrictions

Standard finite element tools provide only the system matrices $\mathbf{G}_{j,j'}$ and $\mathbf{C}_{j,j'}$ in the case $j = j'$. However, also matrices with $j \neq j'$ occur in frame coordinates, see (32). Fortunately, such matrices can be provided by using restrictions and prolongations.

Let $U_0 \subset U_1 \subset \cdots$ be the given sequence of finite element spaces in $H^1(D)$. We denote the restriction of the function

$$f_j = \sum_{k \in \Delta_j^D} f_{j,k} \varphi_{j,k} = \Phi_j \mathbf{f}_j \in U_j$$

to the space U_ℓ, $\ell < j$, by I_j^ℓ. The corresponding discrete operator will be denoted by $\mathbf{I}_j^\ell$, that is

$$I_j^\ell f_j = \Phi_\ell \mathbf{I}_j^\ell \mathbf{f}_j \in U_\ell.$$

Conversely, I_ℓ^j resp. $\mathbf{I}_\ell^j$ denotes the prolongation of $f_\ell = \Phi_\ell \mathbf{f}_\ell \in U_\ell$ onto U_j. Both the application of the restriction $\mathbf{I}_j^\ell$ and the prolongation $\mathbf{I}_\ell^j$ to a vector is of complexity $\mathcal{O}(2^{nj}) \sim \dim U_j$.

Invoking restriction and prolongation we obviously have

$$\mathbf{G}_{j,j'} = \begin{cases} \mathbf{I}_{j'}^j \mathbf{G}_{j',j'}, & j \le j', \\ \mathbf{G}_{j,j} \mathbf{I}_{j'}^j, & j > j'. \end{cases} \tag{33}$$

Since we deal with local operators, the finite element matrices $\mathbf{G}_{j,j}$ have only $\mathcal{O}(1)$ nonzero coefficients per column and row, independently of the level j. Thus, employing (33), the matrix-vector multiplication $\mathbf{G}_{j,j'}\mathbf{x}_j$ can be performed in $\mathcal{O}(2^{n \max\{j,j'\}}) \sim \max\{\dim U_j, \dim U_{j'}\}$ operations, which is order-optimal.

In view of our Galerkin discretization we also need to deal with the sequence of finite element spaces $V_0 \subset V_1 \subset \cdots \subset H^1_{\mathrm{per}}(Y)$ with $\dim V_j \sim 2^{nj}$. Associated prolongations and restrictions will be denoted by $\mathbf{J}_\ell^j$ and $\mathbf{J}_j^\ell$ ($j > \ell$). Obviously, there holds a to (33) analogous expression for the application of the system matrix $\mathbf{C}_{j,j'}$.

4.5. Fast two-factor matrix-vector multiplication

We shall provide a fast two-factor matrix-vector multiplications $\widehat{\mathbf{v}}_j = \widehat{(\mathbf{C}_{j,j} \otimes \mathbf{G}_{j,j})}\widehat{\mathbf{u}}_j$ for matrices and vectors of the form

$$\widehat{\mathbf{C}_{j,j} \otimes \mathbf{G}_{j,j}} = \big[\mathbf{C}_{\ell_2,\ell_2'} \otimes \mathbf{G}_{\ell_1,\ell_1'}\big]_{\ell_1+\ell_2,\ell_1'+\ell_2' \le j}, \quad \widehat{\mathbf{u}} = \big[\widehat{\mathbf{u}}_{\ell_1,\ell_2}\big]_{\ell_1+\ell_2 \le j}. \tag{34}$$

The matrices $\mathbf{G}_{\ell_1,\ell_1'}$ and $\mathbf{C}_{\ell_2,\ell_2'}$ are defined with respect to the two different multiresolution sequences $\{U_j\}_{j\ge 0}$ and $\{V_j\}_{j\ge 0}$. This matrix-vector product can be evaluated in essentially linear complexity $\mathcal{O}(j^3 2^{jn})$ if we apply the algorithm developed in (21; 22) which is based on the following idea. Notice that algorithms which employ similar techniques have been developed in (4; 6; 22; 29; 32).

Let the vector $\widehat{\mathbf{u}}_j = [\widehat{\mathbf{u}}_{\ell_1,\ell_2}]_{\ell_1+\ell_2\le j}$ be blockwise stored in matrix form, i.e. $\widehat{\mathbf{u}}_{\ell_1,\ell_2} \in \mathbb{R}^{|\Delta_{\ell_1}|\times|\Delta_{\ell_2}|}$, and likewise the output vector $\widehat{\mathbf{v}}_j$. Then, for the matrix-vector multiplication (34) we have to compute products of the form

$$\operatorname{vec}(\widehat{\mathbf{v}}_{\ell_1,\ell_2}) = (\mathbf{C}_{\ell_2,\ell_2'} \otimes \mathbf{G}_{\ell_1,\ell_1'}) \operatorname{vec}(\widehat{\mathbf{u}}_{\ell_1',\ell_2'}) \iff \widehat{\mathbf{v}}_{\ell_1,\ell_2} = \mathbf{G}_{\ell_1,\ell_1'} \widehat{\mathbf{u}}_{\ell_1',\ell_2'} \mathbf{C}_{\ell_2,\ell_2'}^\top.$$

Here, vec($\mathbf{X}$) denotes the vectorization of the matrix $\mathbf{X}$ formed by stacking the columns of $\mathbf{X}$ into a single column vector. We achieve the order optimal complexity bound $\mathcal{O}(2^{\max\{\ell_1+\ell_2,\ell_1'+\ell_2'\}n})$ if we perform the multiplications in the following order:

$$\widehat{\mathbf{v}}_{\ell_1,\ell_2} = \begin{cases} \big(\mathbf{G}_{\ell_1,\ell_1'}\widehat{\mathbf{u}}_{\ell_1',\ell_2'}\big)\mathbf{C}_{\ell_2,\ell_2'}^\top, & \ell_1+\ell_2' \le \ell_1'+\ell_2, \\ \mathbf{G}_{\ell_1,\ell_2'}\big(\widehat{\mathbf{u}}_{\ell_1',\ell_2'}\mathbf{C}_{\ell_2,\ell_2'}^\top\big), & \ell_1+\ell_2' > \ell_1'+\ell_2. \end{cases}$$

In accordance with (33), we further use prolongations and restrictions in order to ensure that only standard finite element matrices appear:

Algorithm 1: Fast matrix-vector multiplication $\widehat{\mathbf{v}}_j = (\widehat{\mathbf{C}_{j,j} \otimes \mathbf{G}_{j,j}})\widehat{\mathbf{u}}_j$

Data: Finite Element matrices $\mathbf{G}_{\ell,\ell}$, $\mathbf{C}_{\ell,\ell}$ $(0 \le \ell \le j)$ and input vector $\widehat{\mathbf{u}}_j$

Result: Sparse tensor matrix-vector product $\widehat{\mathbf{v}}_j = (\widehat{\mathbf{C}_{j,j} \otimes \mathbf{G}_{j,j}})\widehat{\mathbf{u}}_j$

begin

- **for** $0 \le \ell_1 + \ell_2 \le j$ **do**
  - initialize $\widehat{\mathbf{w}}_{\ell_1,\ell_2} := \mathbf{0}$;
  - **for** $0 \le \ell_1' + \ell_2' \le j$ **do**
    - **if** $\ell_1 + \ell_2' \le \ell_1' + \ell_2$ **then**
      - **if** $\ell_1 \le \ell_1'$ **then** $\mathbf{y} := \mathbf{I}_{\ell_1'}^{\ell_1}\mathbf{G}_{\ell_1',\ell_1'}\widehat{\mathbf{u}}_{\ell_1',\ell_2'}$; **else**
      - $\mathbf{y} := \mathbf{G}_{\ell_1,\ell_1}\mathbf{I}_{\ell_1'}^{\ell_1}\widehat{\mathbf{u}}_{\ell_1',\ell_2'}$;
      - **if** $\ell_2 \le \ell_2'$ **then** $\mathbf{z} := \mathbf{J}_{\ell_2'}^{\ell_2}\mathbf{C}_{\ell_2,\ell_2'}\mathbf{y}^\top$; **else**
      - $\mathbf{z} := \mathbf{C}_{\ell_2,\ell_2}\mathbf{J}_{\ell_2'}^{\ell_2}\mathbf{y}^\top$;
      - update $\widehat{\mathbf{v}}_{\ell_1,\ell_2} := \widehat{\mathbf{v}}_{\ell_1,\ell_2} + \mathbf{z}^\top$;
    - **else**
      - **if** $\ell_1 \le \ell_1'$ **then** $\mathbf{y} := \mathbf{J}_{\ell_2'}^{\ell_2}\mathbf{C}_{\ell_2,\ell_2'}\widehat{\mathbf{u}}_{\ell_1',\ell_2'}^\top$; **else**
      - $\mathbf{y} := \mathbf{C}_{\ell_2,\ell_2}\mathbf{J}_{\ell_2'}^{\ell_2}\widehat{\mathbf{u}}_{\ell_1',\ell_2'}^\top$;
      - **if** $\ell_2 \le \ell_2'$ **then** $\mathbf{z} := \mathbf{I}_{\ell_1'}^{\ell_1}\mathbf{G}_{\ell_1',\ell_1'}\mathbf{y}^\top$; **else**
      - $\mathbf{z} := \mathbf{G}_{\ell_1,\ell_1}\mathbf{I}_{\ell_1'}^{\ell_1}\mathbf{y}^\top$;
      - update $\widehat{\mathbf{v}}_{\ell_1,\ell_2} := \widehat{\mathbf{v}}_{\ell_1,\ell_2} + \mathbf{z}$;

In case of the matrix-vector product $\mathbf{v}_j^i = (\widehat{\mathbf{b}_j^i \otimes \mathbf{F}_{j,j}^i})\widehat{\mathbf{u}}_j$ with

$$\widehat{\mathbf{b}_j^i \otimes \mathbf{F}_{j,j}^i} = \big[\mathbf{b}_{\ell_2} \otimes \mathbf{F}_{j,\ell_1}^i\big]_{\ell_1+\ell_2\le j}, \quad \widehat{\mathbf{u}}_j = \big[\widehat{\mathbf{u}}_{\ell_1,\ell_2}\big]_{\ell_1+\ell_2\le j}, \quad i = 1,2,\dots,n.$$

we proceed in a similar way. One finds

$$\mathbf{v}_j^i = \sum_{\ell_1+\ell_2\le j} \mathbf{F}_{j,\ell_1}^i \widehat{\mathbf{u}}_{\ell_1,\ell_2} (\mathbf{b}_{\ell_2}^i)^\top = \mathbf{F}_{j,j}^i \left[\sum_{\ell_1=0}^{j} \mathbf{I}_{\ell_1}^j \left(\sum_{\ell_2=0}^{j-\ell_1} \widehat{\mathbf{u}}_{\ell_1,\ell_2} (\mathbf{b}_{\ell_2}^i)^\top \right) \right], \qquad i = 1, 2, \ldots, n.$$

Since the inner sum's complexity is bounded by $\sum_{\ell_2=0}^{j-\ell_1} \mathcal{O}(2^{(\ell_1+\ell_2)n}) = \mathcal{O}(2^{jn})$, only $\mathcal{O}(j2^{jn})$ operations are required to evaluate this expression if one uses the following algorithm:

Algorithm 2: Fast matrix-vector multiplication $\mathbf{v}_j^i = (\widehat{\mathbf{b}_j^i \otimes \mathbf{F}_{j,j}^i})\widehat{\mathbf{u}}_j$

Data: finite element matrices $\mathbf{F}_{j,j}^i$, $\mathbf{b}_\ell^i$ $(0 \le \ell \le j)$ and input vector $\widehat{\mathbf{u}}_j$
Result: matrix-vector product $\mathbf{v}_j^i = (\widehat{\mathbf{b}_j^i \otimes \mathbf{F}_{j,j}^i})\widehat{\mathbf{u}}_j$
begin
  for $0 \le \ell_1 \le j$ **do**
    if $\ell_1 = 0$ **then** $\mathbf{w}_{\ell_1} := \mathbf{0}$; **else** $\mathbf{w}_{\ell_1} := \mathbf{I}_{\ell_1-1}^{\ell_1} \mathbf{w}_{\ell_1-1}$;
    for $0 \le \ell_2 \le j - \ell_1$ **do** update $\mathbf{w}_{\ell_1} := \mathbf{w}_{\ell_1} + \widehat{\mathbf{u}}_{\ell_1,\ell_2} (\mathbf{b}_{\ell_2}^i)^\top$;
  $\mathbf{u}_j^i := \mathbf{F}_{j,j}^i \mathbf{w}_j$;

Finally, the adjoint matrix-vector product $\widehat{\mathbf{v}}_j^i = (\widehat{\mathbf{b}_j^i \otimes \mathbf{F}_{j,j}^i})^\top \mathbf{u}_j$ is computed blockwise:

$$\widehat{\mathbf{v}}_{\ell_1,\ell_2}^i = (\mathbf{F}_{j,\ell_1}^i)^\top \mathbf{u}_j \mathbf{b}_{\ell_2}^i = \Big(\mathbf{I}_{\ell_1}^j (\mathbf{F}_{j,j}^i)^\top \mathbf{u}_j \Big) \mathbf{b}_{\ell_2}^i, \quad i = 1, 2, \ldots, n.$$

We shall first compute the bracket, i.e., the vectors

$$\mathbf{w}_j := (\mathbf{F}_{j,j}^i)^\top \mathbf{u}_j, \qquad \mathbf{w}_{\ell_1} := \mathbf{I}_{\ell_1+1}^{\ell_1} \mathbf{w}_{\ell_1+1}, \quad \ell_1 = j-1, j-2, \ldots, 0.$$

This requires $\sum_{\ell=0}^{j} \mathcal{O}(2^{\ell n}) = \mathcal{O}(2^{jn})$ operations. Next, we compute

$$\widehat{\mathbf{v}}_{\ell_1,\ell_2}^i := \mathbf{w}_{\ell_1} \mathbf{b}_{\ell_2}^i, \quad 0 \le \ell_1 + \ell_2 \le j,$$

which gives additional $\sum_{\ell_1+\ell_2\le j} \mathcal{O}(2^{(\ell_1+\ell_2)n}) = \mathcal{O}(j2^{jn})$ operations. In summary, we arrive at

Algorithm 3: Fast matrix-vector multiplication $\widehat{\mathbf{v}}_j^i = (\widehat{\mathbf{b}_j^i \otimes \mathbf{F}_{j,j}^i})^\top \mathbf{u}_j$

Data: finite element matrices $\mathbf{F}_{j,j}^i$, $\mathbf{b}_\ell^i$ $(0 \le \ell \le j)$ and input vector $\mathbf{u}_j$
Result: matrix-vector product $\widehat{\mathbf{v}}_j^i = (\widehat{\mathbf{b}_j^i \otimes \mathbf{F}_{j,j}^i})^\top \mathbf{u}_j$
begin
  for $j \ge \ell_1 \ge 0$ **do**
    if $\ell_1 = j$ **then** $\mathbf{w}_j := (\mathbf{F}_{j,j}^i)^\top \mathbf{u}_j$; **else** $\mathbf{w}_{\ell_1} := \mathbf{I}_{\ell_1+1}^{\ell_1} \mathbf{w}_{\ell_1+1}$;
    for $0 \le \ell_2 \le j - \ell_1$ **do** $\widehat{\mathbf{v}}_{\ell_1,\ell_2}^i := \mathbf{w}_{\ell_1} \mathbf{b}_{\ell_2}^i$;

We can now combine Algorithms 1–3 to define the efficient matrix-vector multiplication in the conjugate gradient method. Concerning the complexity we conclude essentially linear over-all complexity.

Proposition 4.4. *By using the Algorithms 1–3 the application of the system matrix from* (31) *to a vector* $(\mathbf{u}_{0,j}, \widehat{\mathbf{u}}_{1,j})$ *is of essentially linear complexity. Precisely, only* $\mathcal{O}(j^3 2^{jn})$ *operations are necessary to multiply a vector* $(\mathbf{v}_{0,j}, \widehat{\mathbf{v}}_{1,j})$ *with the system matrix from* (31)*. In the case of* $K > 2$ *scales, the operation count equals* $\mathcal{O}(j^{2K-1} 2^{jn})$ *operations if the matrix-vector multiplication is performed as in (22).*

5. Numerical examples

5.1. An analytical example

We implemented the sparse tensor FEM for a model plane two-scale problem (i.e. $n = 2$, $K = 2$). The two hierarchies (1) used in our numerical experiments were based both on continuous, piecewise linear finite elements (i.e. $d = 2$). For testing and demonstrating our implementation we slightly modify the problem under consideration such that the solution is known analytically. Let D be the unit circle $B_1(0,0)$ and Y the unit square $[0,1]^2$. Consider

$$u_0(\mathbf{x}) = 1 - x_1^2 - x_2^2, \quad u_1(\mathbf{x},\mathbf{y}) = x_1^3 \sin(2\pi y_1)\sin(2\pi y_2),$$
$$A(\mathbf{x},\mathbf{y}) = \alpha(\mathbf{x})\beta(\mathbf{y}) = 1 + \frac{1}{2}\sin(2\pi y_1)\sin(2\pi y_2).$$

Then, the tuple $(u_0, u_1) \in \mathbf{V}$ is the unique solution of the boundary value problem

$$b\big((u_0,u_1),(v_0,v_1)\big) = \int_D \int_Y f(\mathbf{x},\mathbf{y})v_0(\mathbf{x}) + g(\mathbf{x},\mathbf{y})v_1(\mathbf{x},\mathbf{y})d\mathbf{y}d\mathbf{x},$$

where

$$\begin{aligned} f(\mathbf{x},\mathbf{y}) &= 4 + 2\sin(2\pi y_1)\sin(2\pi y_2), \\ g(\mathbf{x},\mathbf{y}) &= 4\pi\big\{x_1\cos(2\pi y_1)\sin(2\pi y_2) + x_2\sin(2\pi y_1)\cos(2\pi y_2)\big\} \\ &\quad + 2\pi^2 x_1^3\big\{\big(4 + 2\sin(2\pi y_1)\sin(2\pi y_2)\big)\sin(2\pi y_1)\sin(2\pi y_2) \\ &\qquad - \cos^2(2\pi y_1)\sin^2(2\pi y_2) - \sin^2(2\pi y_1)\cos^2(2\pi y_2)\big\}. \end{aligned}$$

We emphasize that the only difference to the two-scale homogenization problem (15) consists in the modified right hand side.

The coarse grid triangulation (i.e. level 0) of the unit square Y consists of 18 equal sized triangles. From this the triangulations of the higher levels are successively obtained by uniform mesh refinement of each triangle into four triangles (see Subsection 3.1). Thus, on Y we can use standard finite elements. The number of nodes per level can be found in the second column of Table 1.

level	number of unknowns			energy		energy	
	on D	on Y	in $\widehat{W}_j$	error of $u_{0,j}$		error of $\widehat{u}_{1,j}$	
1	41	36	954	$4.1 \cdot 10^{-1}$	(—)	$8.0 \cdot 10^{-1}$	(—)
2	145	144	5607	$2.1 \cdot 10^{-1}$	(2.0)	$3.8 \cdot 10^{-1}$	(2.1)
3	545	576	29124	$1.8 \cdot 10^{-1}$	(1.1)	$2.1 \cdot 10^{-1}$	(1.8)
4	2304	2304	142209	$8.6 \cdot 10^{-2}$	(2.1)	$1.1 \cdot 10^{-1}$	(1.9)
5	8321	9216	669438	$4.3 \cdot 10^{-2}$	(2.0)	$5.7 \cdot 10^{-2}$	(1.9)
6	33025	36864	3.1 Mio	$2.2 \cdot 10^{-2}$	(2.0)	$2.9 \cdot 10^{-2}$	(2.0)
7	131585	147456	14 Mio	$1.1 \cdot 10^{-2}$	(2.0)	$1.5 \cdot 10^{-2}$	(2.0)
8	525313	589824	62 Mio	$4.9 \cdot 10^{-3}$	(2.2)	$7.4 \cdot 10^{-2}$	(2.0)

Table 1: Approximation errors with respect to the analytical example.

Whereas, the unit circle D is represented exactly by 16 curved patches. The triangulations on higher levels and the associated finite elements are constructed in accordance with Subsection 3.2. The resulting mesh on level 3 is shown in Figure 3. The number of nodes per level can be found in the third column of Table 1, the fourth column contains the number of ansatz functions in the sparse grid space $\widehat{W}_j$.

In our implementation we employ a polygonal approximation of the curved triangles on the finest grid to compute all appearing fine grid integrals. Integrals on the coarser grids are successively computed via restriction from the fine grid components. This ensures optimal computational complexity of the assembly procedure while preserving consistency.

For the given right hand side we computed the numerical solution for the levels $1, 2, \ldots, 8$ and compared it with the analytical solution. The related energy errors $\epsilon_{0,j} := \|u_0 - u_{0,j}\|_{H^1(D)}$ and $\epsilon_{1,j} := \|u_1 - \widehat{u}_{1,j}\|_{L^2(D)\otimes H^1(Y)}$ are

level	1	2	3	4	5	6	7	8
number of iterations	30	33	39	43	46	48	47	47
over-all cpu-time	0 s	1 s	3 s	24 s	181 s	1260 s	2.4 h	17 h

Table 2: Performance with respect to the analytical example.

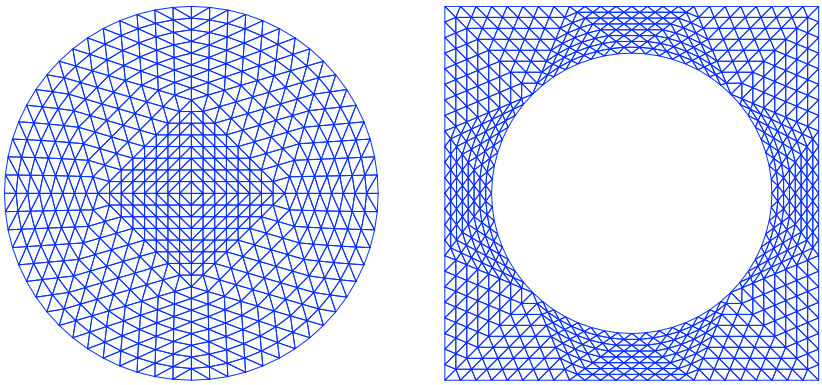

Figure 3: The macroscopic domain D (left) and the unit-cell Y (right) in case of the perforated domain D^ε.

tabulated in the fifth and sixth column of Table 1. The bracketed values contain the ratio of the old and the new error. As one figures out this ratio tends to 2.0 which corresponds essentially linear convergence as predicted in Theorem 4.2.

The number of iterations consumed by the conjugate gradient method can be found in Table 2. The number stays bounded as mentioned in Subsection 4.3. Especially the log-factor in the condition number seems to be quite harmless.

The computing times are also tabulated in Table 2. The scaling exhibits still strong logarithmical factors but it is much better than in case quadratic of complexity. In particular, we emphasize that the 62 million unknowns of the sparse grid space on level 8 correspond to more than 300 000 million unknowns of the full tensor product space. The computation on level 8 requires 4.8 Gigabyte memory and 17 hours computing time.

5.2. Homogenization problem with oscillating coefficient

We shall next be concerned with a homogenization problem with oscillating coefficients and choose as before D as the unit circle $B_1(0,0)$ and Y the unit square $[0,1]^2$. We consider the coefficient

$$A(\mathbf{x},\mathbf{y}) = \alpha(\mathbf{x})\beta(\mathbf{y}) = (1+x_1^2+x_2^2)\left(1+\frac{3}{4}\cos(2\pi y_1)\right)\left(1+\frac{3}{4}\cos(2\pi y_2)\right)$$

and the right hand side $f(\mathbf{x}) = 4$. Since the domains D and Y and thus the number of unknowns are the same as in the previous example, the computational performance is nearly the same as in Table 1.

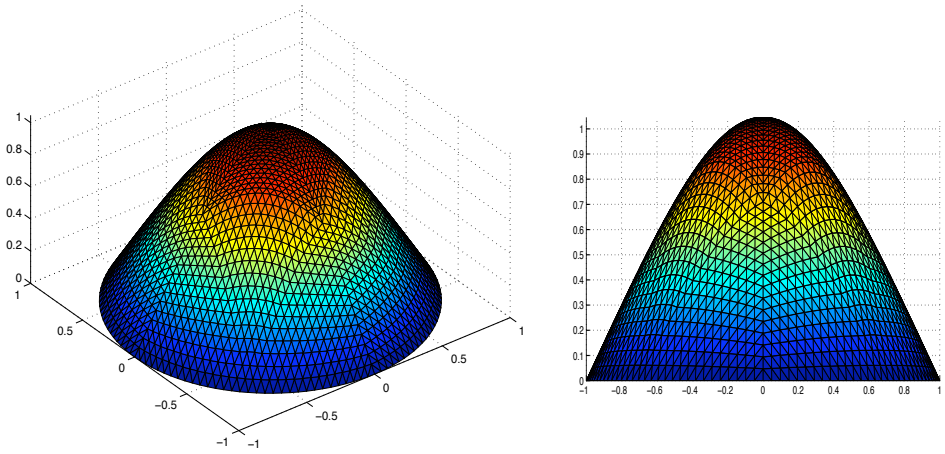

Figure 4: The approximate homogenized solution $u_{0,j}$ in case of an oscillating coefficient.

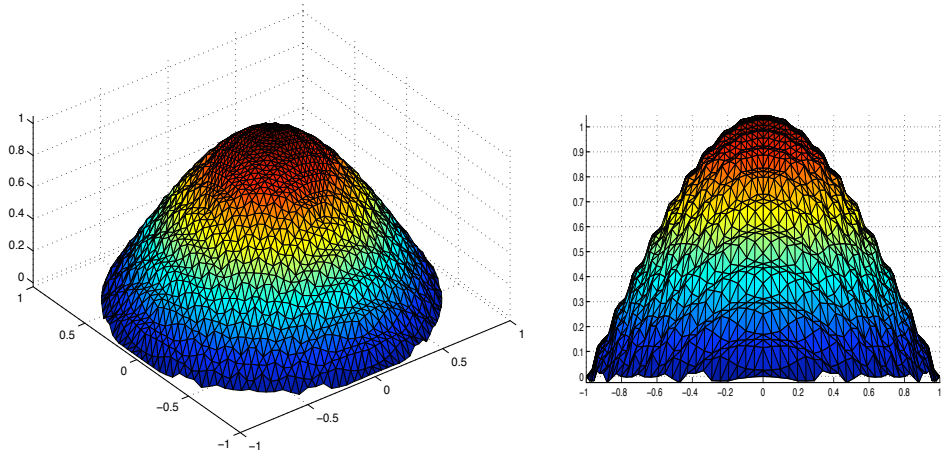

Figure 5: The approximate two-scale solution $u_{0,j} + \varepsilon \widehat{u}_{1,j}\left(\cdot, \frac{\cdot}{\varepsilon}\right)$ for $\varepsilon = 0.1$.

The approximate solution $u_{0,j}$ on the discretization level $j = 4$ is depicted in Figure 4. The associated approximate two-scale solution $u_{0,j}(\mathbf{x}) + \varepsilon \widehat{u}_{1,j}(\mathbf{x}, \mathbf{x}/\varepsilon)$ is plotted in Figure 5 for the choice $\varepsilon = 0.1$. However, according to (23), convergence of the two-scale solution might only be ensured in terms of the estimate

$$\left\| \nabla_{\mathbf{x}} u^\varepsilon - \nabla_{\mathbf{x}} u_{0,j} - w_j^\varepsilon(\mathbf{x}) \right\|_{L^2(D)} = \mathcal{O}(\sqrt{\varepsilon} + j h_j)$$

where the quantity v_j^ε is derived via a post-processing by applying the "folding" operator:

$$w_j^\varepsilon(\mathbf{x}) = \int_Y \nabla_{\mathbf{y}} \widehat{u}_{1,j} \left(\varepsilon \left\lfloor \frac{\mathbf{x}}{\varepsilon} \right\rfloor + \varepsilon \mathbf{z}, \frac{\mathbf{x}}{\varepsilon} - \left\lfloor \frac{\mathbf{x}}{\varepsilon} \right\rfloor \right) d\mathbf{z}, \quad \mathbf{x} \in D.$$

Herein, $\lfloor \mathbf{x}/\varepsilon \rfloor$ denotes the "integer" part of $\mathbf{x}/\varepsilon$ with respect to Y.

5.3. A homogenization problem in a perforated domain

We now consider the situation that $Y \subset [0,1]^n$ with strict inclusion. Then the sets Γ_{int}, $\partial Y \backslash \partial([0,1]^n)$ and $\Gamma_{\text{int}}^\varepsilon := \partial D^\varepsilon \backslash \partial D$ are nonempty. We refer to Figure 1 where we depict a perforated circle with circular perforations of size ε. For such situations, the problem formulation requires the imposition of boundary conditions on $\Gamma_{\text{int}}^\varepsilon$. On $\Gamma_{\text{int}}^\varepsilon$ we impose, following (12; 13), Robin boundary conditions on Γ_{int}, i.e.,

$$\mathbf{n} \cdot A \nabla u + h \varepsilon u^\varepsilon = \varepsilon g^\varepsilon \text{ on } \Gamma_{\text{int}}^\varepsilon$$

with $h \geq 0$ being a non-negative real constant. As is shown in (12; 13), the two-scale convergence approach is also applicable in this case (albeit under the provision of a uniform with respect to ε in $H^1(D^\varepsilon)$ Poincaré inequality).

We therefore choose again the unit circle $B_1(0,0)$ as macroscopic domain D and the unit cell is defined as a square with hole: $Y := [0,1]^2 \setminus B_{3/8}(0.5, 0.5)$. The unit cell is parametrized via 16 curved patches. The resulting mesh on level 3 is depicted on the right hand side of Figure 3. The further setting is $A(\mathbf{x}, \mathbf{y}) = 1$, $f(\mathbf{x}) = 4$, $h = 0$ and $g(\mathbf{x}) = 0$. The approximate homogenized solution $u_{0,j}$ on level $j = 4$ is depicted in Figure 6.

In Table 3 we tabulated the number of nodes per level as well as the number of ansatz functions in the sparse grid space $\widehat{W}_j$. The required number of iterations of the conjugate gradient method are found in the fifth column of Table 3, the cpu-times are found in the sixth column. The performance is quite similar to that of the previous examples.

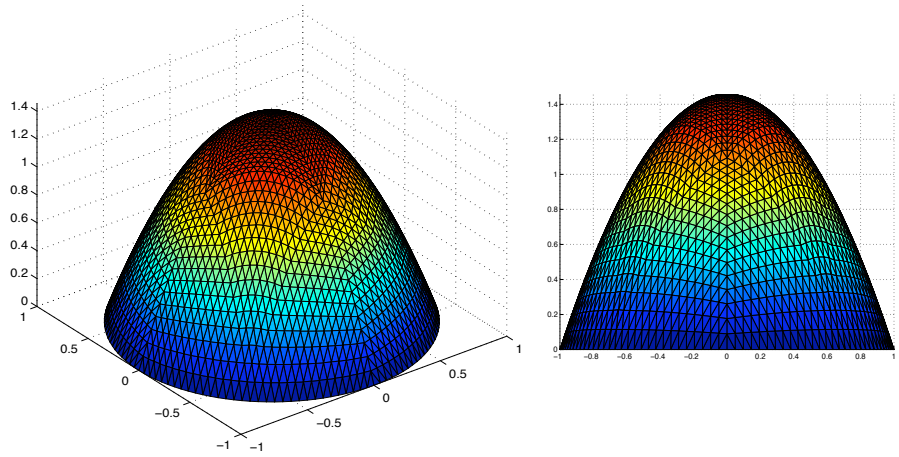

Figure 6: The approximate homogenized solution $u_{0,j}$ in case of a perforated circle.

level	number of unknowns			number of	over-all
	on D	on Y	in $\widehat{W}_j$	iterations	cpu-time
1	41	47	1313	22	0 s
2	145	175	7400	32	1 s
3	545	671	37198	38	4 s
4	2113	2623	177267	44	32 s
5	8321	10367	819735	47	230 s
6	33025	41215	3.7 Mio	50	1627 s
7	131585	164351	17 Mio	52	3.6 h

Table 3: Computational performance associated with the perforated circle.

6. Concluding remarks

We remark in closing that, in the present paper, we have shown the construction of sparse tensor product FE discretizations of anisotropic, elliptic one-scale limiting problems resulting from reiterated homogenization of elliptic multiscale problems with any finite number $K \geq 2$ of separated scales. The proposed construction achieves, up to logarithmic terms, optimal convergence rates whenever a standard FE (one-scale) basis and a multilevel preconditioner of BPX type is available. The explicit construction of wavelet Finite Elements is not required in the present approach. Numerical examples and implementations were detailed for (finite superpositions of) separable conductivities. We hasten to add, however, that the algorithms presented

here are also applicable to the general, nonseparable setting, if suitable numerical quadratures (which will necessarily be of sparse tensor type) are employed. Their numerical analysis and implementation, however, exceed the format of the present paper and will be considered elsewhere.

1 A. Abdulle and C. Schwab. Heterogeneous Multiscale FEM for Diffusion Problems on Rough Surfaces. *Multiscale Modeling and Simulation: A SIAM Interdisciplinary Journal* **3** (2005) 195–220.

2 G. Allaire. Homogenization and two-scale convergence. *SIAM J. Math. Anal.* **23** (1992) 1482–1518.

3 G. Allaire and M. Briane. Multiscale convergence and reiterated homogenization. *Proc. Roy. Soc. Edin.* **126A** (1996) 297–342.

4 R. Balder. Adaptive Verfahren für elliptische und parabolische Differentialgleichungen auf dünnen Gittern. PhD thesis, Institut für Informatik, TU München, 1994.

5 A. Bensoussan, J.-L. Lions, and G. Papanicolaou. *Asymptotic Analysis for Periodic Structures*. North-Holland, Amsterdam, 1978.

6 R. Balder and C. Zenger. The solution of multidimensional real Helmholtz equations on sparse grids. *SIAM J. Sci. Comput.* **17** (1996) 631–646.

7 J. Bramble, J. Pasciak, and J. Xu. Parallel multilevel preconditioners. *Math. Comput.* **55** (1990) 1–22.

8 H.J. Bungartz and M. Griebel. Sparse Grids. *Acta Numerica* **13** (2004) 147–269.

9 O. Christiansen. *An Introduction to Frames and Riesz Bases*. Applied and Numerical Harmonic Analysis. Birkhäuser Boston Inc., Boston, 2002.

10 P.G. Ciarlet. *The Finite Element Method for Elliptic Problems*. Elsevier, North-Holland, 1978.

11 D. Cioranescu, A. Damlamian, and G. Griso. *The periodic unfolding method in homogenization. SIAM J. Appl. Math.* **40** (2008) 1585–1620.

12 D. Cioranescu, P. Donato, and R. Zaki. The periodic unfolding method in perforated domains. *Portugaliae Mathematica* **63** (2006) 467–496.

13 D. Cioranescu, P. Donato, and R. Zaki. Periodic unfolding and Robin problems in perforated domains. *Comptes Rendus Mathematique* **342** (2006) 469–474.

14 S. Dahlke, M. Fornasier, T. Raasch, R. Stevenson, and M. Werner. Adaptive Frame Methods for Elliptic Operator Equations: The Steepest Descent Approach. *IMA J. Numer. Math.* **27** (2007) 717–740.

15 W. Dahmen. Wavelet and multiscale methods for operator equations. *Acta Numerica* **6** (1997) 55–228.

16 I. Daubechies. *Ten lectures on wavelets*. CBMS-NSF Regional Conference Series in Applied Mathematics, vol. 61. SIAM, Philadephia, 1992.

17 M. Griebel. Multilevel algorithms considered as iterative methods on semidefinite systems. *SIAM J. Sci. Comput.* **15** (1994) 547–565.

18 M. Griebel. *Multilevelmethoden als Iterationsverfahren über Erzeugendensystemen.* Teubner Skripten zur Numerik. B.G. Teubner, Stuttgart, 1994.

19 M. Griebel and P. Oswald. On additive Schwarz preconditioners for sparse grid discretizations. *Numer. Math.* **66** (1994) 449–463.

20 M. Griebel and P. Oswald. Tensor product type subspace splittings and multilevel iterative methods for anisotropic problems. *Adv. Comput. Math.* **4** (1995) 171–206.

21 H. Harbrecht. A finite element method for elliptic problems with stochastic input data. *Appl. Numer. Math.* **60** (2010) 227–244.

22 H. Harbrecht, R. Schneider, and C. Schwab. Multilevel frames for sparse tensor product spaces. *Numer. Math.* **110** (2008) 199–220.

23 V.H. Hoang and C. Schwab. High-dimensional finite elements for elliptic problems with multiple scales. *Multiscale Model. Simul.* **3** (2005) 168–194.

24 V. Jikov, S. Kozlov, and O. Oleinik. *Homogenization of Differential Operators and Integral Function.* Springer, Berlin, 1994.

25 E.F. Kaasschieter. Preconditioned conjugate gradients for solving singular systems. *J. of Comput. Appl. Math.* **24** (1988) 265–275.

26 G. Nguetseng. A general convergence result related to the theory of homogenization. *SIAM J. Math. Anal.* **20** (1989) 608–629.

27 P. Oswald. *Multilevel finite element approximation. Theory and applications.* Teubner Skripten zur Numerik. B.G. Teubner, Stuttgart, 1994.

28 T. von Petersdorff and C. Schwab. Sparse wavelet methods for operator equations with stochastic data. *Applications of Mathematics* **51** (2006) 145–180.

29 A. Pfaffinger. Funktionale Beschreibung und Parallelisierung von Algorithmen auf dünnen Gittern. PhD thesis, Institut für Informatik, TU München, 1997.

30 C. Schwab. High-dimensional finite elements for elliptic problems with multiple and stochastic data. in *Proc. Intern. Congress of Mathematicians*, vol. III, pp. 727–734. Higher Education Press Beijing, P.R.C., 2002.

31 C. Schwab and R. Stevenson. Adaptive Wavelet Algorithms for Elliptic PDEs on Product Domains *Math. Comput.* **77** (2008) 71–92.

32 C. Schwab and R. Todor. Sparse finite elements for elliptic problems with stochastic loading. *Numer. Math.* **95** (2003) 707–734.

33 C. Schwab and R. Todor. Sparse finite elements for stochastic elliptic problems-higher order moments. *Computing* **71** (2003) 43–63.

34 C. Schwab and R. Todor. Karhunen-Loève approximation of random fields by generalized fast multipole methods. *J. Comp. Phys.* **217** (2006) 100–122.

35 R. Stevenson. Adaptive solution of operator equations using wavelet frames. *SIAM J. Numer. Anal.* **41** (2003) 1074–1100.

36 L. Tartar. *The General Theory of Homogenization. A Personalized Introduction.* Lecture Notes of the Unione Matematica Italiana, vol. 7, Springer, 2010.

37 C. Zenger. Sparse grids. Parallel algorithms for partial differential equations, in *Proceedings of the 6th GAMM-Seminar, Kiel/Germany, 1990*, pp. 241–251, Notes Numer. Fluid Mech., vol. 31. Vieweg, Germany, 1991.

Research Reports

No.	Authors/Title
10-34	*H. Harbrecht and Ch. Schwab* Sparse tensor finite elements for elliptic multiple scale problems
10-33	*K. Grella and C. Schwab* Sparse tensor spherical harmonics approximation in radiative transfer
10-32	*P. Kauf, M. Torrilhon and M. Junk* Scale-induced closure for approximations of kinetic equations
10-31	*M. Hansen* On tensor products of quasi-Banach spaces
10-30	*P. Corti* Stable numerical scheme for the magnetic induction equation with Hall effect
10-29	*H. Kumar* Finite volume methods for the two-fluid MHD equations
10-28	*S. Kurz and H. Heumann* Transmission conditions in pre-metric electrodynamics
10-27	*F.G. Fuchs, A.D. McMurry, S. Mishra and K. Waagan* Well-balanced high resolution finite volume schemes for the simulation of wave propagation in three-dimensional non-isothermal stratified magneto-atmospheres
10-26	*U.S. Fjordholm, S. Mishra and E. Tadmor* Well-balanced, energy stable schemes for the shallow water equations with varying topography
10-25	*U.S. Fjordholm and S. Mishra* Accurate numerical discretizations of non-conservative hyperbolic systems
10-24	*S. Mishra and Ch. Schwab* Sparse tensor multi-level Monte Carlo finite volume methods for hyperbolic conservation laws with random intitial data
10-23	*J. Li, J. Xie and J. Zou* An adaptive finite element method for distributed heat flux reconstruction
10-22	*D. Kressner* Bivariate matrix functions